PERGAMON

International Journal of Solids and Structures 39 (2002) 145–157

INTERNATIONAL JOURNAL OF SOLIDS and STRUCTURES

www.elsevier.com/locate/ijsolstr

Generic unfolding of the thermoelastic contact instability

D.D. Quinn [a,*], J.A. Pelesko [b]

[a] *Department of Mechanical Engineering, The University of Akron, Akron, OH 44325-3903, USA*
[b] *School of Mathematics, Georgia Institute of Technology, Atlanta, GA 30332, USA*

Received 13 October 2000; in revised form 5 June 2001

Abstract

The classic model of a one-dimensional thermoelastic rod suspended between a hot and cold wall is revisited. In this model, the rod is held in place at the cold end, while at the hot end it is allowed to separate from or make contact with the wall. When the model includes the contact and gap dependent thermal boundary condition known as the Barber condition it serves to illustrate the well-known thermoelastic contact instability. All previous studies of this instability have focused upon the symmetric case where, as a control parameter is varied, the system undergoes a pitchfork bifurcation. That is, a new pair of linearly stable steady-state solutions bifurcate symmetrically from a previously unique solution which has changed from stable to unstable. Here, it is shown that this behavior is not generic. Rather, for typical contact resistance functions, a fold bifurcation is encountered. This represents a generic unfolding of the classic pitchfork bifurcation and contains the pitchfork as a special case.

Keywords: Thermoelastic contact; Barber condition; Multiple scales; Unfolding

1. Introduction

In their now classic paper, Barber et al. (1980), investigated the effect of thermal contact boundary conditions in a one-dimensional model of a thermoelastic rod. Motivated by the numerous applications in which thermoelastic contact problems arise (see e.g. Lee and Barber (1993), Richmond et al. (1990) and Srinivasan and France (1985)), and directed by Barber's earlier realization that the solution of such problems posed difficulties (Barber, 1978), the trio demonstrated that when the physically realistic boundary condition introduced by Barber (1978), was imposed, the one-dimensional model underwent a bifurcation. In particular, as a control parameter proportional to the applied temperature gradient in the model was varied, the system underwent a bifurcation from a unique linearly stable steady-state solution to multiple solutions with alternating stability. In their analysis, a symmetry in the contact resistance function was assumed. As a result, the bifurcation uncovered was of the pitchfork type.

Since the original study, numerous authors have continued the investigation of the thermoelastic contact instability. Various authors have explored the effect of geometry by for example considering contact

* Corresponding author. Tel.: +1-330-972-6302; fax: +1-330-972-6027.
E-mail addresses: quinn@uakron.edu (D.D. Quinn), pelesko@math.gatech.edu (J.A. Pelesko).

0020-7683/01/$ - see front matter
PII: S0020-7683(01)00148-2

between a layer and a half plane (Yeo and Barber, 1991), or a strip and a rigid wall, (Yeo and Barber, 1995), or between two cylinders in cylindrical geometry, (Zhang and Barber, 1993; Noda, 1984, 1985, 1987). Other authors have focused on the technologically important case of thermoelastic instability in sliding contact (see e.g. Lee and Barber (1993), Barber et al. (1985), Azarkhin and Barber (1986), Johnson et al. (1988) and Zagrodzki (1990)), while still others have explored the effect of changing material properties (Zhang and Barber, 1990; Joachim-Ajao and Barber, 1998; Li and Barber, 1998). The mathematical theory of thermoelastic contact models has also undergone development with several authors investigating existence and uniqueness questions (Andrews et al., 1993; Rivera and Racke, 1998; Lin, 1997; Shi and Shillor, 1993). Still, other authors have returned to plumb the depths of one-dimensional models. In Barber (1981), multiple coupled one-dimensional rods were considered as an approximation to three-dimensional bodies. In Barber and Zhang (1988) and Cheng and Shillor (1993), the case of two one-dimensional rods in contact was shown to produce oscillatory solutions. Finally, in Pelesko (1999, 2001), the second author developed a nonlinear stability theory for one-dimensional thermoelastic contact models.

Despite the intense interest in these problems, all of the studies mentioned above and to the author's knowledge all such studies, have failed to mention the fact that the pitchfork bifurcation is not generic. That is, in order to obtain a bifurcation which characterizes the thermoelastic contact instability, it is necessary to vary some parameter in the problem. Usually, this parameter is proportional to an applied thermal gradient (Barber et al., 1980), or perhaps to the sensitivity of the contact resistance function (Pelesko, 1999, 2001). However, the contact resistance function, R, is always the key factor as this is what determines how rapidly heat conduction through contacting surfaces changes as a function of contact pressure or distance between those surfaces. As the bifurcation parameter is varied, the multiplicity of steady states undergoes a change according as related changes in the contact resistance function. An assumption of symmetry for the reciprocal contact resistance function, i.e., $F = 1/(1 + R)$, leads to a bifurcation of pitchfork type. However, there is no physical reason to expect such symmetry and in fact, in general, one expects quite the opposite.

In this paper, we investigate the implications of asymmetry in the reciprocal contact resistance function. We show that the pitchfork bifurcation is not the generic bifurcation associated with the thermoelastic contact instability. Rather, we show that the instability is more appropriately characterized in terms of a fold bifurcation, of which the pitchfork bifurcation is a special case. We begin, in Section 2, with a statement of the one-dimensional model to be considered. We discuss the contact resistance function and physically reasonable assumptions about its nature. We review the linear theory for this model and highlight differences which arise due to an asymmetric reciprocal contact resistance function. In Section 3, we develop a weakly nonlinear stability theory for the generic case. We employ the method of multiple scales or "two timing" in the development of an asymptotic scheme which incorporates stabilizing nonlinear terms into the linear theory (see e.g. Kevorkian and Cole (1996) and Matkowsky (1970)). Finally, we use this theory to discuss the history dependence and dynamic evolution of solutions to the one-dimensional rod model.

2. The model

We consider a one-dimensional thermoelastic rod suspended between two rigid walls as pictured in Fig. 1. We assume the rod possesses constant thermal and elastic material properties, is homogeneous and isotropic and that uncoupled quasi-static thermoelasticity is valid. Our governing equations in dimensionless forms are:

$$\frac{\partial \theta}{\partial t} = \frac{\partial^2 \theta}{\partial x^2}, \quad 0 < x < 1, \tag{1a}$$

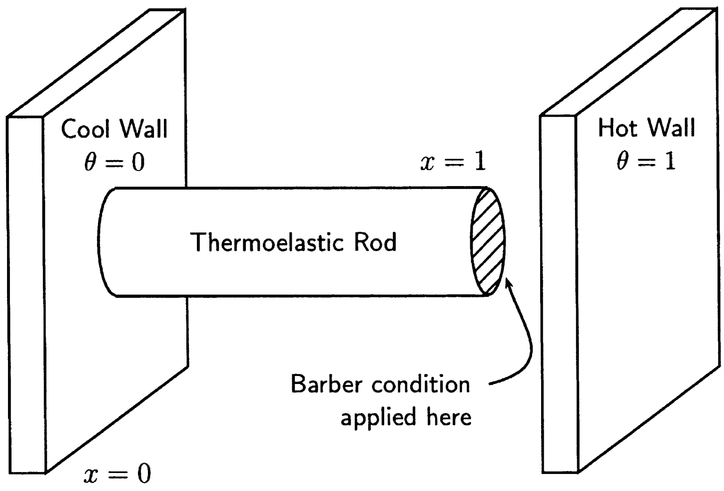

Fig. 1. Sketch of the model geometry.

$$\theta(0, t) = 0, \tag{1b}$$

$$R(\eta)\frac{\partial\theta}{\partial x}(1, t) = 1 - \theta(1, t), \tag{1c}$$

$$\eta = -\mu \int_0^1 \theta(\zeta, t)\ \mathrm{d}\zeta. \tag{1d}$$

Here, θ is dimensionless temperature, and the coupled thermoelastic problem has been reduced to a purely thermal one by solving the elastic equations exactly. The remaining remnant of the elastic problem is the variable η which measures the gap size between the rod and the right hand wall during periods of separation ($\eta > 0$) and contact pressure during periods of contact ($\eta < 0$). $R(\eta)$ is the contact resistance function and μ is a dimensionless version of the coefficient of thermal expansion and is proportional to the temperature difference between the right and left walls. Note that the rod is assumed to be held at a fixed cold temperature at the left, Eq. (1b), while at the hot right wall we have imposed the Barber condition, Eq. (1c). For a full derivation of these equations, including scaling and the exact solution to the elastic problem, the reader is referred to Pelesko (1999, 2001).

2.1. The contact resistance function

The key to understanding the thermoelastic instability lies within the contact resistance function $R(\eta)$. While the concept of contact resistance is intuitive, its experimental and mathematical characterization is rather difficult. Intuition corresponds to a mental picture of heat transfer between contacting surfaces. First, if two bodies are not in contact, heat transfer between them will take place due to radiation and convection, while once they make contact heat transfer will be dominated by conduction. Hence, that R should be a function of gap size or contact is easy to see. Once contact is made, the heat transfer by conduction is a function of the surface area of contact. Due to asperities on the microlevel, the actual surface area of contact is but a fraction of the nominal contact area. Further, as the contact pressure between two surfaces is increased, elastic or plastic deformation occurs leading to an increase in the actual surface area of contact. Hence, it is also intuitive that R should be a function of contact pressure. How to determine the actual functional form of R is not nearly so clear as the intuition behind it, despite its critical role in evolution of thermoelastic systems (Andrews et al., 1993). Due to the technological importance of this concept, much research has been directed towards its understanding. The reader is referred to Sridhar and Yovanovich (1994), and Lambert and Fletcher (1997a) for reviews of this complex field. Also, Williamson and Majumdar (1992) and Lambert and Fletcher (1997b) serve as introductions to the modeling and experimental verification of models of the contact resistance function. A perusal of these articles reveals that there is little agreement as to the functional form of R and perhaps more importantly that this functional form can be a strong function of the contacting materials and surface roughness. For our macroscopic study however, it is sufficient to extract several properties that any R must possess. We summarize them as:

Definition 2.1. A contact resistance function $R(\eta)$ is a function satisfying:

- $R(\eta) \geqslant 0 \quad \forall\ \eta$;
- $\lim_{\eta\to-\infty} R(\eta) = 0$;
- $\lim_{\eta\to\infty} R(\eta) = \infty$;
- $R(\eta)$ is a monotonically increasing function of η.

The limiting behavior of R is best understood by recalling that $\eta \to -\infty$ corresponds to infinite contact pressure, while $\eta \to \infty$ corresponds to infinite gap. As it will also be convenient to work with the reciprocal contact resistance function, defined by

$$F(\eta) = \frac{1}{1 + R(\eta)}. \tag{2}$$

We summarize the properties of F as well:

Definition 2.2. A reciprocal contact resistance function, $F(\eta)$, also called the contact conductance, is a function satisfying:

- $F(\eta) \geqslant 0 \quad \forall\ \eta$;
- $\lim_{\eta\to-\infty} F(\eta) = 1$;
- $\lim_{\eta\to\infty} F(\eta) = 0$;
- $F(\eta)$ is a monotonically decreasing function of η.

Notice, that no smoothness properties have been assumed for R or F. In general, neither need be smooth. In fact, at the transitional point between contact and separation, $\eta = 0$, there is often a discontinuity in the slope of $R(\eta)$. However, in the analysis which follows, we shall assume differentiability of R and F as necessary.

2.2. Linear theory

In this section we review the linear theory for our model, Eqs. (1a)–(1d), and point out precisely which assumptions lead to a pitchfork bifurcation versus a fold type bifurcation. To begin, the steady-state solution is determined by setting time derivative to zero in Eq. (1a) and integrate the resulting ordinary differential equation, yielding:

$$\theta^*(x) = A^*x + B^*. \tag{3}$$

Applying the boundary condition at $x = 0$, Eq. (1b), implies that $B^* = 0$. Application of the boundary condition at $x = 1$, Eq. (1c), yields:

$$A^* = \frac{1}{1 + R(\eta^*)}, \qquad \eta^* = -\frac{\mu}{2} A^*, \tag{4}$$

and solutions to this equation determine the equilibrium value of A^*. Note that in terms of the contact conductance, this equilibrium condition may be rewritten as:

$$A^* = F(\eta^*), \qquad \eta^* = -\frac{\mu}{2} A^*. \tag{5}$$

The equilibrium solutions are easily uncovered by graphical analysis. In Fig. 2, we plot the left and right hand sides of Eq. (5) to illustrate this fact. Given the previous definition of the reciprocal contact resistance $F(\eta)$, it is straightforward to show that at least one intersection exists. In Fig. 2, we have purposefully sketched these equilibrium conditions to produce a single intersection. It is easy to imagine however, that if the slope of F at the intersection were steeper, multiple intersections could occur. Such a situation is pictured in Fig. 3. This is precisely the bifurcation uncovered by Barber et al. (1980). A closer look at this situation is in order. We assume that at a specific value of μ, say $\mu = \mu_0$, there exists an intersection and hence an equilibrium solution at $\eta^* = \eta_0$. As pictured in Fig. 3, the new solutions occur symmetrically about η_0. That is, one new solution satisfies $\eta^* > \eta_0$ while the other satisfies $\eta^* < \eta_0$. Such a scenario will be the

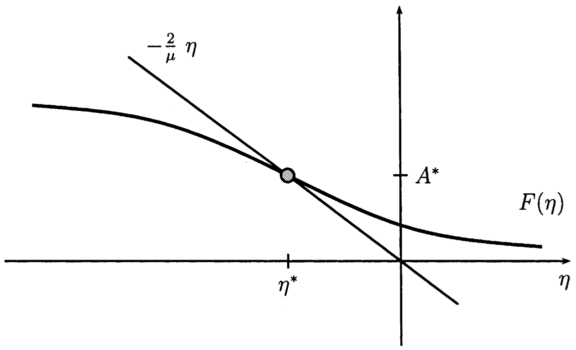

Fig. 2. Sketch of the left and right hand sides of the steady-state equation.

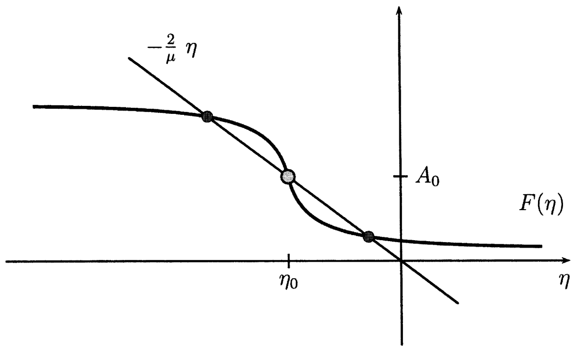

Fig. 3. Sketch of the left and right hand sides of the steady-state equation showing multiple intersections positioned symmetrically about $\eta^* = \eta_0$.

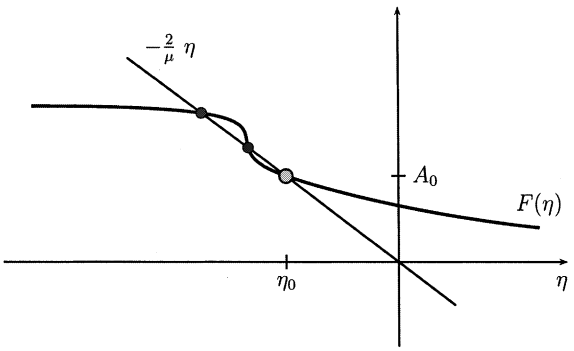

Fig. 4. Sketch of the left and right hand sides of the steady-state equation showing multiple nonsymmetric intersections. Notice that in this figure both equilibria which arise from the bifurcation appear on one side of $\eta^* = \eta_0$.

case if the intersection at $\eta^* = \eta_0$ is an inflection point for F. This corresponds to a pitchfork bifurcation. But, why must this be the case? The transition could in fact occur as pictured in Fig. 4, with the new solutions asymmetrically distributed about $\eta^* = \eta_0$, or in fact both new solutions might appear above or below $\eta^* = \eta_0$!

To clarify further, we study this bifurcation locally by expanding $F(\eta^*)$ in a Taylor series about $\eta^* = \eta_0$, where η_0 is assumed to be an equilibrium solution which occurs for $\mu = \mu_0$. Retaining up to cubic terms yields:

$$F(\eta^*) \sim F(\eta_0) + F'(\eta_0)(\eta^* - \eta_0) + F''(\eta_0)\frac{(\eta^* - \eta_0)^2}{2} + F'''(\eta_0)\frac{(\eta^* - \eta_0)^3}{6}. \tag{6}$$

Now, using Eq. (6) in Eq. (5) and solving for η^*, yields either $\eta^* = \eta_0$, as expected, or two new solutions:

$$\eta^* = \eta_0 - \frac{3F_0''}{2F_0'''} \pm \sqrt{\left(\frac{3F_0''}{2F_0'''}\right)^2 - \frac{12}{\mu_0 F_0'''}\left(1 + \frac{\mu_0 F_0'}{2}\right)}, \tag{7}$$

with:

$$F_0^i \equiv \left.\frac{\mathrm{d}^i F}{\mathrm{d}\eta^i}\right|_{\eta=\eta_0}.$$

In terms of A^*, these solutions are represented as:

$$A^* = A_0 + \frac{3F_0''}{\mu_0 F_0'''} \pm \sqrt{\left(\frac{3F_0''}{\mu_0 F_0'''}\right)^2 - \frac{48}{\mu_0^3 F_0'''}\left(1 + \frac{\mu_0 F_0'}{2}\right)}.$$

Here the quantity $(\mu_0 F_0')/2$ is a convenient bifurcation parameter controlling the number of equilibria. Physically, it represents the sensitivity of the contact conductance at the steady-state solution $\theta^*(x) = A_0 x$. Now the unfolding of the bifurcation becomes clear. We have three solutions for η^* when the argument of the square root in Eq. (7) is positive. If $F_0'' = 0$, then η_0 is an inflection point for F and the bifurcation occurs at $(\mu_0 F_0')/2 = -1$. The bifurcation diagram for different values of F_0'' is depicted in Fig. 5.

Next, we investigate the linear stability of the steady solutions $\theta^*(x) = A^* x$. Accordingly we seek a solution to Eqs. (1a)–(1d) in the form:

$$\theta(x,t) = A^* x + \phi(x)\mathrm{e}^{-\lambda^2 t}, \tag{8}$$

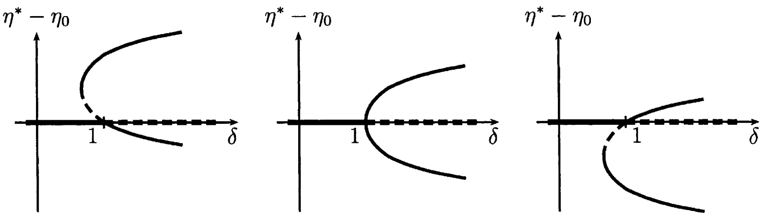

Fig. 5. Bifurcation diagram for different values of F_0'', with $\delta \equiv -(\mu_0 F_0')/2$. Stable branches of equilibria are indicated by a solid curve, while unstable branches are shown dashed.

where $|\phi(x)| \ll 1$. Inserting this ansatz into our governing equations, expanding the nonlinear terms in Taylor series, and omitting quadratic and higher order terms in ϕ, we obtain the eigenvalue problem:

$$\frac{\mathrm{d}^2\phi}{\mathrm{d}x^2} + \lambda^2\phi = 0, \tag{9a}$$

$$\phi(0) = 0, \tag{9b}$$

$$(1 - F(\eta^*))\phi'(1) + \mu F'(\eta^*) \int_0^1 \phi(\zeta)\, \mathrm{d}\zeta + F(\eta^*)\phi(1) = 0. \tag{9c}$$

Notice that we have written this in terms of the contact conductance F. This linear eigenvalue problem has a solution $\phi(x)$ when λ satisfies:

$$(1 - F(\eta^*))\lambda\cos(\lambda) + \mu F'(\eta^*)\left(\frac{1 - \cos(\lambda)}{\lambda}\right) + F(\eta^*)\sin(\lambda) = 0. \tag{10}$$

The solutions of this equation in conjunction with Eq. (8) determine the stability of the perturbation ϕ; if $\mathrm{Re}(\lambda^2) > 0$ (<0), then the steady-state solution is linearly stable (unstable). This characteristic equation, in an equivalent form, was studied by Barber et al. (1980); we do not repeat his analysis here. Rather, we simply note that in our notation, the results of Barber indicate that the equilibrium $\theta^*(x) = A^*x$ is asymptotically stable (unstable) if $F'(\eta^*) > -2/\mu$ ($<$) and is marginally stable for $F'(\eta^*) = -2/\mu$. As the stability boundary always occurs for $F'(\eta^*) = -2/\mu$, independent of $F''(\eta^*)$, we may deduce linear stability for equilibria through a graphical analysis of Figs. 2–4. If $F(\eta)$ crosses the line defined by $(-2/\mu)\eta$ from left to right, the resulting equilibrium point is stable. However, if the crossing is from right to left, the equilibrium point is unstable. The stability results are summarized in Fig. 5.

3. A nonlinear theory

In the previous section we found the steady-state solutions for our model and investigated their linear stability. The linear analysis, developed from Eqs. (7) and (10) and summarized in Fig. 5, indicates that as a suitable bifurcation parameter is varied, a fold bifurcation occurs generically, with the pitchfork bifurcation identified by previous authors as a special case. The quantity F'' was used as the unfolding parameter. In addition, it was seen that equilibria are unstable for $F' < -2/\mu$. When an equilibrium solution is unstable, the linear theory predicts that any infinitesimal perturbation will grow exponentially with time. Clearly, the linear theory is expected to be valid only for a short time. In this section, we extend our analysis using the method of multiple scales to account for the effects of nonlinearities in the governing equations. That is, we investigate the behavior of solutions *near* a marginally stable equilibrium through introduction of the scalings:

$$
\begin{aligned}
F_0' &= -\frac{2}{\mu_0} + \varepsilon^2 f_0', \\
F_0'' &= \varepsilon f_0'', \\
F_0''' &= f_0'''.
\end{aligned}
\tag{11}
$$

For $\varepsilon = 0$, the equilibrium at $\eta^* = \eta_0$ is marginally stable, so that ε characterizes the distance of the system to the bifurcation described above. For $\varepsilon f_0'' = 0$, recall from Eq. (6) that $\eta^* = \eta_0$ is an inflection point of $F(\eta)$ and, as described in Eq. (7), the system exhibits a pitchfork bifurcation as the quantity $\varepsilon^2 f_0'$ passes through zero. For $f_0'' \neq 0$, $\eta^* = \eta_0$ is no longer an inflection point of $F(\eta)$, and we find that the bifurcation is of the fold type as illustrated in Fig. 5. Moreover, the fold bifurcation occurs at $\mu = \mu_0 + \Delta$, where:

$$
\Delta = \frac{-\varepsilon^2 \mu_0^2 \left[\frac{3(f_0'')^2}{16 f_0'''} - \frac{f_0'}{2} \right]}{1 + \varepsilon^2 \mu_0 \left[\frac{3(f_0'')^2}{16 f_0'''} - \frac{f_0'}{2} \right]},
$$

and represents the generic unfolding of the pitchfork bifurcation as seen in Fig. 5, with the unfolding parameter being f_0''.

We begin the nonlinear analysis by expanding the bifurcation parameter μ as a series in ε:

$$
\mu = \mu_0 + \varepsilon\mu_1 + \varepsilon^2\mu_2 + \varepsilon^3\mu_3 + \cdots.
$$

In what follows the system will be assumed to be neutrally stable when $\mu = \mu_0$, that is, for $\varepsilon = 0$. Thus ε characterizes the distance, in terms of the bifurcation parameter μ, from neutral stability. A multiple scales analysis requires that time is stretched as:

$$
t_0 = t, \quad t_1 = \varepsilon t, \quad t_2 = \varepsilon^2 t, \quad \ldots,
$$

and both θ and η are expanded in ε:

$$
\begin{aligned}
\theta(x,t) &= \theta_0(x) + \varepsilon\theta_1(x,t) + \varepsilon^2\theta_2(x,t) + \cdots, \\
\eta(t) &= \eta_0 + \varepsilon\eta_1(t) + \varepsilon^2\eta_2(t) + \cdots.
\end{aligned}
$$

Finally, the reciprocal contact resistance function $F(\eta)$ is expanded in ε about η_0, and with the introduction of the scalings defined in Eq. (11), to $\mathcal{O}(\varepsilon^3)$ this becomes:

$$
F(\eta) = F_0 + (F_0'\eta_1)\varepsilon + (F_0'\eta_2)\varepsilon^2 + \left(f_0'\eta_1 + \frac{f_0''}{2}\eta_1^2 + \frac{f_0'''}{6}\eta_1^3 + F_0'\eta_3 \right)\varepsilon^3 + \cdots,
$$

so that f_0', f_0'', and f_0''' characterize the Barber condition near the marginally stable state. These expansions are introduced into Eqs. (1a)–(1d) and terms are collected at each order in ε:

$$
\begin{aligned}
&\mathcal{O}(\varepsilon^0) \\
&\frac{\partial\theta_0}{\partial t_0} = \frac{\partial^2\theta_0}{\partial x^2}, \quad \theta_0(0,t) = 0, \\
&(1 - F_0)\frac{\partial\theta_0}{\partial x}(1,t) = F_0(1 - \theta_0(1,t)), \\
&\eta_0 = -\mu_0 \int_0^1 \theta_0(x,t)\,\mathrm{d}x,
\end{aligned}
$$

$\mathcal{O}(\varepsilon^1)$

$$\frac{\partial\theta_0}{\partial t_1}+\frac{\partial\theta_1}{\partial t_0}=\frac{\partial^2\theta_1}{\partial x^2},\quad \theta_1(0,t)=0,$$

$$(1-F_0)\frac{\partial\theta_1}{\partial x}(1,t)+F_0\theta_1(1,t)=(F_0'\eta_1)\left(\frac{\partial\theta_0}{\partial x}(1,t)+1-\theta_0(1,t)\right),$$

$$\eta_1=-\mu_0\int_0^1\theta_1(x,t)\,\mathrm{d}x-\mu_1\int_0^1\theta_0(x,t)\,\mathrm{d}x,$$

$\mathcal{O}(\varepsilon^2)$

$$\frac{\partial\theta_0}{\partial t_2}+\frac{\partial\theta_1}{\partial t_1}+\frac{\partial\theta_2}{\partial t_0}=\frac{\partial^2\theta_2}{\partial x^2},\quad \theta_2(0,t)=0,$$

$$(1-F_0)\frac{\partial\theta_2}{\partial x}(1,t)+F_0\theta_2(1,t)=(F_0'\eta_1)\left(\frac{\partial\theta_1}{\partial x}(1,t)-\theta_1(1,t)\right)+(F_0'\eta_2)\left(\frac{\partial\theta_0}{\partial x}(1,t)+1-\theta_0(1,t)\right),$$

$$\eta_2=-\mu_0\int_0^1\theta_2(x,t)\,\mathrm{d}x-\mu_1\int_0^1\theta_1(x,t)\,\mathrm{d}x-\mu_2\int_0^1\theta_0(x,t)\,\mathrm{d}x,$$

$\mathcal{O}(\varepsilon^3)$

$$\frac{\partial\theta_0}{\partial t_3}+\frac{\partial\theta_1}{\partial t_2}+\frac{\partial\theta_2}{\partial t_1}+\frac{\partial\theta_3}{\partial t_0}=\frac{\partial^2\theta_3}{\partial x^2},\quad \theta_3(0,t)=0,$$

$$(1-F_0)\frac{\partial\theta_3}{\partial x}(1,t)+F_0\;\theta_3(1,t)=(F_0'\eta_1)\left(\frac{\partial\theta_2}{\partial x}(1,t)-\theta_2(1,t)\right)+(F_0'\eta_2)\left(\frac{\partial\theta_1}{\partial x}(1,t)-\theta_1(1,t)\right)$$
$$+\left(f_0'\eta_1+\frac{f_0''}{2}\eta_1^2+\frac{f_0'''}{6}\eta_1^3+F_0'\eta_3\right)\left(\frac{\partial\theta_0}{\partial x}(1,t)+1-\theta_0(1,t)\right),$$

$$\eta_3=-\mu_0\int_0^1\theta_3(x,t)\,\mathrm{d}x-\mu_1\int_0^1\theta_2(x,t)\,\mathrm{d}x-\mu_2\int_0^1\theta_1(x,t)\,\mathrm{d}x-\mu_3\int_0^1\theta_0(x,t)\,\mathrm{d}x.$$

The multiple scales analysis proceeds by solving these equations in turn at each order in ε. Therefore we obtain a series of linear variational equations. To ensure that solutions are nonsecular, that is, they do not grow in time, we remove secular terms by appropriate choices which ultimately determine the nonlinear stability of the system.

To lowest order, the dominant solution is given as $\theta_0(x,t)=A_0x$, where:

$$A_0=F(\eta_0)=\text{constant},\qquad \eta_0=-\frac{\mu_0}{2}A_0,$$

with $0<A_0<1$. Therefore using this lowest order solution one can identify A_0, the thermal gradient, with η_0, the nondimensional variable related to the thermal expansion.

At the next order we again assume a separable solution. We find that the eigenvalues of the characteristic equation are nonpositive, so that all solutions decay exponentially, with the exception of the solution of the form:

$$\theta_1(x,t)=A_1(t_1,t_2,t_3,\ldots)x.$$

The coefficient A_1 is allowed to vary on timescales of order $t_1=\varepsilon t$ and slower. In the sequel we will denote this dependence as $A_1(t_1)$. The notation will explicitly contain only the *fastest* timescale dependence, the remaining slower timescales are suppressed for clarity. This solution corresponds to the eigenvalue at the origin and leads to the solvability equation:

$$\left[1+\frac{\mu_0}{2}F_0'\right]A_1+\left[\frac{\mu_1}{2}F_0'\right]A_0=0.$$

This equation is satisfied for all values of A_1 provided:

$$F_0'=-\frac{2}{\mu_0},\qquad \mu_1=0.$$

The first of these conditions reflects the neutral stability of the point about which the nonlinear analysis is being performed, that is, $\mu=\mu_0$. The second reveals that a nontrivial amplitude A_1 at $\mathcal{O}(\varepsilon)$ requires that the detuning of the system from neutral stability be $o(\varepsilon)$.

At $\mathcal{O}(\varepsilon^2)$ we find the general solution is of the form:

$$\theta_2(x,t)=A_2(t_1)x+\frac{\partial A_1}{\partial t_1}\frac{x^3}{6},$$

whose solvability equation is satisfied for all values of A_1 provided:

$$\frac{\partial A_1}{\partial t_1}=0,\qquad \mu_2=0.$$

With this, A_1 does not vary on the t_1 timescale, that is, $A_1=A_1(t_2)$.

Finally, at $\mathcal{O}(\varepsilon^3)$, the solvability equation reduces to:

$$0=\left[\frac{5-4A_0}{12}\right]\left(\frac{\partial A_2}{\partial t_1}+\frac{\partial A_1}{\partial t_2}\right)+\left\{\frac{\mu_0}{2}f_0'A_1-\left(\frac{\mu_0}{2}\right)^2\frac{f_0''}{2}A_1^2+\left(\frac{\mu_0}{2}\right)^3\frac{f_0'''}{6}A_1^3-\frac{\mu_3}{\mu_0}A_0\right\},$$

which is satisfied for $\partial A_2/\partial t_1=0$, and:

$$\frac{\partial A_1}{\partial t_2}=-\frac{12}{(5-4A_0)}\left\{\frac{\mu_0}{2}f_0'A_1-\left(\frac{\mu_0}{2}\right)^2\frac{f_0''}{2}A_1^2+\left(\frac{\mu_0}{2}\right)^3\frac{f_0'''}{6}A_1^3-\frac{\mu_3}{\mu_0}A_0\right\}.$$

This evolution equation for A_1 determines the long-time behavior of the amplitude of $\theta_1(x,t)$, the $\mathcal{O}(\varepsilon)$ correction to the base solution. This equation can be written as:

$$\frac{\partial A_1}{\partial t_2}=c\left[\left(\frac{48A_0}{\mu_0^4f_0'''}\right)\mu_3-\left(\frac{24f_0'}{\mu_0^2f_0'''}\right)A_1+\left(\frac{6f_0''}{\mu_0f_0'''}\right)A_1^2-A_1^3\right],$$

where:

$$c=\frac{\mu_0^3f_0'''}{4(5-4A_0)}.$$

We note that provided $f_0'''>0$ all solutions remain bounded in time (recall $0<A_0<1$), and the parameter c can be scaled away by an appropriate positive scaling of t_2. Without loss of generality we assume that $c=1$, so that the evolution of A_1 is determined by the Landau–Stuart equation:

$$\frac{\partial A_1}{\partial t_2}=\beta_0\mu_3-\beta_1A_1+\beta_2A_1^2-A_1^3, \tag{12}$$

where:

$$\beta_0=\frac{48A_0}{\mu_0^4f_0'''},\qquad \beta_1=\frac{24f_0'}{\mu_0^2f_0'''},\qquad \beta_2=\frac{6f_0''}{\mu_0f_0'''}.$$

The qualitative behavior of $A_1(t_2)$ as the bifurcation parameter μ_3 is varied is determined by the parameters β_0, β_1, and β_2. The equilibrium points determined by this evolution equation are identical to the nontrivial equilibria described by Eq. (7).

Previous analyses which have focused on the symmetric pitchfork bifurcation can be recovered through the assumptions $\beta_0 = \beta_2 = 0$. We see that $\beta_0\mu_3 \neq 0$ arises through the physically realistic choice of μ as the bifurcation parameter. Recall that μ is the nondimensional coefficient of thermal expansion and is proportional to the temperature difference between the hot and cold walls. The assumption of a nonsymmetric contact conductance about the marginally stable solution leads to $\beta_2 \neq 0$. Each of these effects breaks the pitchfork bifurcation described in Barber et al. (1980) and Pelesko (2001), leading to a generic fold bifurcation. Finally, we note that the bifurcation parameter used in these previous studies, defined as δ in Fig. 5 is equivalent to β_1 defined above.

4. Discussion

We have revisited the classic model of a one-dimensional thermoelastic rod suspended between a hot and cold wall. In contrast to earlier studies of this model (Barber et al., 1980; Barber, 1981; Barber and Zhang, 1988; Cheng and Shillor, 1993; Pelesko, 1999, 2001), in this work we have allowed for a more general representation of the contact conductance function F near the point of neutral stability, including asymmetry, and have considered μ, the nondimensional temperature difference across the walls as the relevant bifurcation parameter. These previous works assumed a symmetric form for the contact conductance near the bifurcation and consequently the bifurcation parameter described the functional form of the contact conductance near the point of neutral stability. The major result of this paper is that these extensions, that is, the asymmetry and choice of the bifurcation parameter, implied that the generic bifurcation associated with the thermoelastic instability is a *fold* type bifurcation, instead of the pitchfork bifurcation identified earlier (Pelesko, 1999, 2001). We note that this generic behavior contains the classic pitchfork bifurcation as a special case.

After introducing the model and making physically realistic assumptions about the contact resistance function, we reviewed and extended the linear theory for this system. We found that the structure of the equilibrium solutions was controlled by F_0'', the second derivative of the contact conductance function. In particular, when $F_0'' = 0$, we recover the pitchfork bifurcation as $\delta = -(\mu_0 F_0')/2$ varies, while when $F_0'' \neq 0$, the equilibria which arise from the bifurcation are nonsymmetrically positioned about the trivial solution. This is illustrated in Fig. 5. The linear stability of the trivial equilibrium solution shown in Fig. 5 was then investigated and the stability characteristics were shown to be in agreement with those expected from the pitchfork case.

Next, we developed a nonlinear stability theory for the generic fold bifurcation. To accomplish this, we used the method of multiple scales or two timing to obtain a uniformly valid asymptotic expansion of the solution. This technique yielded the following asymptotic approximation to the solution:

$$\theta(x,t) \sim A_0 x + \varepsilon A_1(\varepsilon^2 t)x + \cdots. \tag{13}$$

Here, A_1 satisfies the amplitude or Landau–Stuart equation:

$$\frac{\partial A_1}{\partial t_2} = \beta_0\mu_3 - \beta_1 A_1 + \beta_2 A_1^2 - A_1^3, \tag{14}$$

where μ_3 represents the $\mathcal{O}(\varepsilon^3)$ detuning from the point of neutral stability. We note that all other terms of $\mathcal{O}(\varepsilon)$ in the asymptotic expansion decay as time tends to infinity. Hence, the limiting behavior of $\theta(x,t)$ is given by:

$$\lim_{t\to\infty} \theta(x,t) \sim A_0 x + \varepsilon\left[\lim_{t\to\infty} A_1(\varepsilon^2 t)\right] x. \tag{15}$$

Examination of Eq. (14) reveals the implications of our assumption of asymmetry as well as the choice for the bifurcation parameter. In particular, the presence of the A_1^2 term depends upon F_0'' while the constant term is linear in μ_3. When both F_0'' and μ_3 vanish, we recover the Landau equation obtained in the nonlinear stability theory of Pelesko (2001), and an accompanying pitchfork bifurcation as β_1 varies. In contrast when either of these quantities are nonzero, we obtain a generic fold bifurcation. Hence, in addition to controlling the equilibrium structure, we see that the asymmetry in F effects the nonlinear behavior and hence the history dependence and dynamics of solutions. Moreover, the contact conductance as well as the choice of the bifurcation parameter influence the history dependence and dynamics of solutions for the original thermoelastic contact problem.

Finally, we suggest that the analysis above may be fruitfully applied to other thermoelastic contact problems. In particular, it would be interesting to examine the implications of asymmetry in the contact resistance function for multidimensional or multirod problems. We invite the reader to further ponder the implications of the generic unfolding for other thermoelastic contact problems.

References

Andrews, K.T., Shi, P., Shillor, M., Wright, S., 1993. Thermoelastic contact with Barber heat-exchange condition. Applied Mathematics and Optimization 28 (1), 11–48.

Azarkhin, A., Barber, J.R., 1986. Thermoelastic instability for the transient contact problem of two sliding half-planes. ASME Journal of Applied Mechanics 53, 565–572.

Barber, J.R., 1978. Contact problems involving a cooled punch. Journal of Elasticity 8, 409–423.

Barber, J.R., 1981. Stability of thermoelastic contact for the Aldo model. ASME Journal of Applied Mechanics 48, 555–558.

Barber, J.R., Beamond, T.W., Waring, J.R., Pritchard, C., 1985. Implications of thermoelastic instability for the design of brakes. ASME Journal of Tribology 107, 206–210.

Barber, J.R., Dundurs, J., Comninou, M., 1980. Stability considerations in thermoelastic contact. ASME Journal of Applied Mechanics 47, 871–874.

Barber, J.R., Zhang, R., 1988. Transient behavior and stability for the thermoelastic contact of two rods of dissimilar materials. International Journal of Mechanical Sciences 30, 691–704.

Cheng, C.C.-A., Shillor, M., 1993. Numerical solutions to the problem of thermoelastic contact of two rods. Mathematical and Computer Modelling 17, 53–71.

Joachim-Ajao, D., Barber, J.R., 1998. Effect of material properties in certain thermoelastic contact problems. ASME Journal of Applied Mechanics 65, 889–893.

Johnson, R.R., Dow, T.A., Zhang, Y.Y., 1988. Thermoelastic instability in elliptic contact between two sliding surfaces. ASME Journal of Tribology 110, 80–86.

Kevorkian, J., Cole, J.D., 1996. Multiple Scale and Singular Perturbation Methods. Springer, New York.

Lambert, M.A., Fletcher, L.S., 1997a. Review of models for thermal contact conductance of metals. Journal of Thermophysics and Heat Transfer 11, 129–140.

Lambert, M.A., Fletcher, L.S., 1997b. Thermal contact conductance of spherical rough metals. ASME Journal of Heat Transfer 119, 684–690.

Lee, K., Barber, J., 1993. Frictionally excited thermoelastic instability in automotive disk breaks. ASME Journal of Tribology 115, 607–614.

Li, C., Barber, J.R., 1998. Stability of thermoelastic contact of two layers of dissimilar materials. Journal of Thermal Stresses 20, 169–184.

Lin, Y., 1997. A nonlocal parabolic system modelling axially symmetric thermoelastic contact of two discs. Journal of Mathematical Analysis and Applications 210, 39–57.

Matkowsky, B.J., 1970. A simple nonlinear dynamic stability problem. Bulletin of the American Mathematical Society 76, 620–625.

Noda, N., 1984. Transient thermoelastic contact problem in a long, circular cylinder. Journal of Thermal Stresses 7, 135–147.

Noda, N., 1985. Transient thermoelastic contact problem in a short-length circular cylinder. Journal of Thermal Stresses 8, 413–424.

Noda, N., 1987. Transient thermoelastic contact problem in a cylinder with a position dependent heat transfer coefficient. Journal of Thermal Stresses 10, 57–69.

Pelesko, J.A., 1999. Nonlinear stability considerations in thermoelastic contact. ASME Journal of Applied Mechanics 66, 109–116.

Pelesko, J.A., 2001. Nonlinear stability, thermoelastic contact and the Barber condition. ASME Journal of Applied Mechanics 68, 28–33.

Richmond, O., Hector Jr., L.G., Fridy, J.M., 1990. Growth instability during nonuniform directional solidification of pure metals. ASME Journal of Applied Mechanics 57, 529–536.

Rivera, J.E.M., Racke, R., 1998. Multidimensional contact problems in thermoelasticity. SIAM Journal on Applied Mathematics 58, 1307–1337.

Shi, P., Shillor, M., 1993. A quasistatic contact problem in thermoelasticity with a radiation condition for the temperature. Journal of Mathematical Analysis and Applications 172, 147–165.

Sridhar, M.R., Yovanovich, M.M., 1994. Review of elastic and plastic contact conductance models: Comparison with experiment. Journal of Thermophysics and Heat Transfer 8, 633–640.

Srinivasan, M.G., France, D.M., 1985. Nonuniqueness in steady state heat transfer in prestressed duplex tubes – Analysis and case history. ASME Journal of Applied Mechanics 48, 555–558.

Williamson, M., Majumdar, A., 1992. Effect of surface deformations on contact conductance. ASME Journal of Heat Transfer 114, 802–810.

Yeo, T., Barber, J.R., 1991. Stability of thermoelastic contact of a layer and a half-plane. Journal of Thermal Stresses 14, 371–388.

Yeo, T., Barber, J.R., 1995. Stability of a semi-infinite strip in thermoelastic contact with a rigid wall. International Journal of Solids and Structures 32, 553–567.

Zagrodzki, P., 1990. Analysis of thermomechanical phenomena in multidisc clutches and brakes. Wear 140, 291–308.

Zhang, R., Barber, J.R., 1990. Effect of material properties on the stability of static thermoelastic contact. ASME Journal of Applied Mechanics 57, 365–369.

Zhang, R., Barber, J.R., 1993. Transient thermoelastic contact and stability of two thin-walled cylinders. Journal of Thermal Stresses 16, 31–54.